

The MAGIC highlights of the gamma ray binary LS I +61 303

T. Jogler^{*}, N. Puchades[†], O. Blanch Bigas[†], V. Bosch-Ramon[‡], J. Cortina[†], J. Moldón[‡],
J. M. Paredes[‡], M. A. Perez-Torres[§], M. Ribó[‡], J. Rico[¶], D. F. Torres^{||}, and V. Zabalza[‡]
on behalf the MAGIC collaboration

^{*}Max-Planck-Institut für Physik, D-80805 München, Germany

[†]IFAE, Edifici Cn., Campus UAB, E-08193 Bellaterra, Spain

[‡]Universitat de Barcelona (ICC/IEEC), E-08028 Barcelona, Spain

[§]Inst. de Astrofísica de Andalucía (CSIC), E-18080 Granada, Spain

[¶]ICREA, E-08010 Barcelona, Spain

^{||} Institut de Ciències de l'Espai (IEEC-CSIC), E-08193 Bellaterra, Spain

Abstract. The discovery of emission of TeV gamma rays from X-ray binaries has triggered an intense effort to better understand the particle acceleration, absorption, and emission mechanisms in compact binary systems. Here we present the pioneering effort of the MAGIC collaboration to understand the very high energy emission of the prototype system LS I +61 303. We report on the variable nature of the emission from LS I +61 303 and show that this emission is indeed periodic. The system shows regular outburst at TeV energies in phase $\phi = 0.6 - 0.7$ and detect no signal at periastron ($\phi \sim 0.275$). Furthermore we find no indication of spectral variation along the orbit of the compact object and the spectral energy distribution is compatible with a simple power law with index $\Gamma = 2.6 \pm 0.2_{stat} \pm 0.2_{sys}$. To answer some of the open questions concerning the emission process of the TeV radiation we conducted a multiwavelength campaign with the MAGIC telescope, *XMM-Newton*, and *Swift* in September 2007. We detect a simultaneous outburst at X-ray and TeV energies, with the peak at phase 0.62 and a similar shape at both wavelengths. A linear fit to the strictly simultaneous X-ray/TeV flux pairs provides $r = 0.81^{+0.06}_{-0.21}$. Here we present the observations and discuss the implications of the obtained results to the emission processes in the system.

Keywords: gamma rays: observations — gamma rays: individual (LS I +61 303) — gamma rays: binaries

I. INTRODUCTION

LS I +61 303 is a high mass X-ray binary system located at 2.0 ± 0.2 kpc from us [1]. The system contains a rapidly rotating early type B0 Ve star with a stable equatorial decretion disk and mass loss, and a compact object with a mass between 1 and 4 M_{\odot} orbiting it every ~ 26.5 d (see [2], [3], [4], and references therein). Although LS I +61 303 has been classified as a microquasar [5], VLBA images obtained during a full orbital cycle show an elongated morphology that rotates as a function of the orbital phase [6]. Later VLBA images show repeating morphologies at the same orbital phases, suggesting that the milliarcsecond morphology depends

only on the orbital phase [7]. This may be consistent with a model based on the interaction between the relativistic wind of a young non-accreting pulsar and the wind/decretion disk of the stellar companion [8]

LS I +61 303 shows periodic non-thermal radio outbursts on average every $P_{orb} = 26.4960 \pm 0.0028$ d, with the peak of the radio emission shifting between phase 0.45 and 0.95, using $T_0 = \text{JD } 2,443,366.775$, in a superorbital period of 1667 ± 8 d [9]. According to the most precise orbital parameters periastron takes place at phase 0.275 and the eccentricity of the orbit is 0.537 ± 0.034 [4].

LS I +61 303 has been observed several times in the X-ray domain (see [10] and references therein). It generally displays X-ray outbursts, between orbital phase 0.4 and 0.8.

At very high energy (VHE) gamma rays LS I +61 303 has been extensively studied by MAGIC [11], [12] and VERITAS [13]. The lack of a systematic behavior from cycle to cycle at X-ray energies, and the occurrence of short-term variability, prevents to establish a X-ray/TeV correlation from the comparison of non-simultaneous data [14].

Here we report about the highlights of the MAGIC VHE gamma ray observation and present our strictly simultaneous TeV and X-ray observations of LS I +61 303.

II. VHE GAMMA RAY OBSERVATIONS AND DATA ANALYSIS

The MAGIC telescope located on the Canary Island of La Palma (28.75°N , 17.86°W , 2225 m a.s.l.). Its essential parameters are a 17 m diameter segmented mirror of parabolic shape, an f/D of 1.05 and an hexagonally shaped camera of 576 hemispherical photo multiplier tubes with a field of view of 3.5° diameter. MAGIC can detect gamma rays from 60 GeV to several TeV. Its energy resolution is $\Delta E = 20\%$ above energies of 200 GeV. The current sensitivity is 1.6% of the Crab Nebula flux for a 5σ detection in 50 h of observation time. The improvement compared to previous sensitivity was achieved by installing new 2 GHz FADCs [15].

The data analysis was carried out using the standard MAGIC analysis and reconstruction software [16] and is in detail described in [11], [12], [17].

The TeV observations were performed in three distinct observational campaigns (OC hereafter). OC I, which lead to the discovery of LS I +61 303 as a γ -ray emitter, was performed from September 2005 to March 2006 and covered 6 orbital periods of LS I +61 303 with a total effective observation time of 54 h. OC II covered only 4 orbital periods but with a much denser sampling compared to OC I and resulted in an effective observation time of 112 h taken in September 2006 to December 2006. Finally OC III data were taken from 4th - 21st September 2007 with an effective observation time of 54 h. The range of zenith angles for all observations was $[32^\circ, 55^\circ]$, although most of the data had zenith angle below 44° . More details about these observations can be found in [11], [12], [17].

III. THE VHE GAMMA RAY TEMPORAL BEHAVIOR

The light curve in OC I and OC II is derived above $E > 400$ GeV and for OC III above $E > 300$ GeV due to the improved sensitivity.

The most pronounced feature in the light curve is the high flux level in the phase range ϕ 0.6-0.7. In this phase range is almost every time the highest flux (during one orbital cycle) measured.

Since the real value of the periastron passage is yet debated the averaged flux value between the phase bin 0.2-0.3 can be used as an upper limit to the emission at periastron. Thus the flux must be less than $F(E > 400\text{GeV}) = 2.2 \times 10^{-12} \text{cm}^{-2} \text{s}^{-1}$ at the 95% confidence level.

Additional significant fluxes are measured during phase 0.5-0.6 in OC II and OC I. In OC II and in OC III additional high fluxes are evident in the phase range 0.8-1.0. In OC II only a single significant measurement occurs at $\phi = 0.84$, while the emission spreads over more nights in OC III yielding an averaged significant ($\sim 5\sigma$) signal in the phase range 0.8-1.0 at the level of $(5.2 \pm 1.0) \times 10^{-12} \text{cm}^{-2} \text{s}^{-1}$. This flux level is compatible with the $2\text{-}\sigma$ upper limit we obtain for the OC II [12]. The higher sensitivity both due to improved hardware and longer observation times can sufficiently explain the non detection in OC II.

We performed a test for periodicity applying the Lomb-Scargle [18] method. The data from OC I and OC II are used and the light curve is binned in intervals of $\Delta t = 15$ min to assure that each measurement has the same error and thus can be treated equal. To evaluate the complementary cumulative probability function we performed a monte carlo simulation by generating 10^6 random generated light curves (from gaussian white noise) with the same sampling as the LS I +61 303 data. For each of the 10^6 light curves the Lomb-Scargle periodogram is calculated and from the maximum peak distribution of all periodograms the complementary cumulative probability density function (cCPF) is computed. The periodogram obtained from the LS I +61 303 light curve is shown together with the background event periodogram in Fig.1. A highly

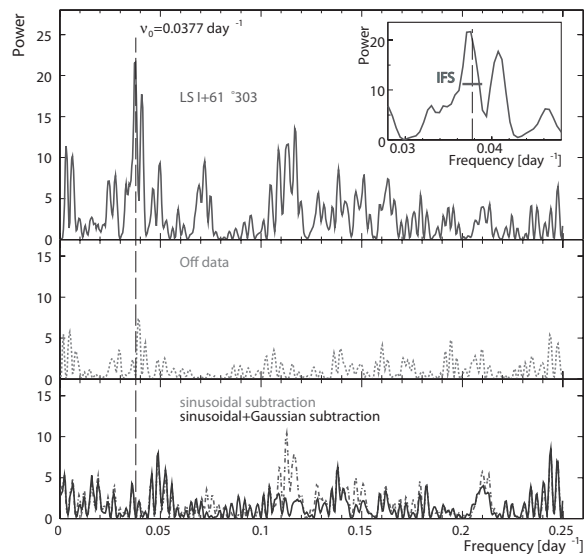


Fig. 1: Lomb-Scargle periodogram over the combined 2005 and 2006 campaigns of LS I +61 303 data (upper panel) and simultaneous background data (middle panel). In the lower panel we show the periodograms after subtraction of a sinusoidal signal at the orbital period (dotted) and a sinusoidal plus a Gaussian wave form (solid). Vertical dashed line corresponds to the orbital frequency. Inset: zoom around the highest peak, which corresponds to the orbital frequency (0.0377d^{-1}). Its post-trial probability is nearly 10^{-7} . The IFS is also shown.

significant peak is found at a period of $P = 26.8 \pm 0.2$ d with a false alarm probability of $\sim 10^{-7}$ in very good agreement with the orbital period of the system. Our test proves that the VHE emission from LS I +61 303 is periodic modulated with the orbital period. A very detailed description of our periodicity analysis and the treatment of possible systematic effects of the method can be found in [12].

IV. THE VHE SPECTRAL BEHAVIOR

The flux measured from LS I +61 303 in individual nights is usually not high enough to obtain significant spectra. The only exception is the main emission peak in phase ϕ 0.6-0.7. We obtained several spectra for individual phase bins in each OC. All spectral energy distributions are compatible with simple power laws. Within the errors all obtained fit parameters are compatible with each other and with the most significant measured spectrum $\frac{dF}{dE} = \frac{(1.2 \pm 0.4_{\text{stat}} \pm 0.3_{\text{sys}}) \cdot 10^{-12}}{\text{TeV cm}^2 \text{s}} \left(\frac{E}{1 \text{TeV}}\right)^{-2.7 \pm 0.4_{\text{stat}} \pm 0.2_{\text{sys}}}$. So no significant spectral variation could be found. We investigated the less significant flux measurements by calculating a hardness ration (HR), which we define as the ratio of the integral flux between 400 GeV and 900 GeV and above 900 GeV. We do not find any correlation between the HR and the flux level.

V. MULTIWAVELENGTH CAMPAIGN

Multiwavelength observations during OC II (see [7]) yielded no correlation between the radio and the TeV emission of LS I +61 303. Hints of correlated X-ray/TeV emission have been found based on non-simultaneous data taken more than six hours [12] and one day apart in these observations. Here we report only on the strictly simultaneous data taken in 2007.

A. X Ray observations

We observed LS I +61 303 with *XMM-Newton* during seven runs from 2007 September 4 to 11, amounting to a total observation time of 104.3 ks. The data were processed using the version 8.0.0 of the *XMM-Newton* Science Analysis Software (SAS). Known hot or flickering pixels were removed using the standard SAS tasks. Further cleaning to remove from the dataset periods of high background reduced the net total good exposure times to 67.0 and 92.6 ks for the pn and MOS detectors, respectively.

Source spectra were extracted from a $\sim 70''$ radius circle centered on the source (PSF of $15''$) while background spectra were taken from a number of source-free circles with $\sim 150''$ radius. The extracted spectra were analyzed with XSpec v12.3.1 [19]. An absorbed power-law function yielded satisfactory fits for all observations. Unabsorbed fluxes in the 0.3–10 keV range were computed from the spectral fits.

Additional observations of 2–5 ks each (total 28.5 ks) were obtained with the *Swift*/XRT from 2007 September 11 to 22. The total observation time was 28.5 ks. The *Swift* data were processed using the FTOOLS task `xrtpipeline`. The spectral analysis procedures were the same as those used for the *XMM-Newton* data, but fixing the hydrogen column density to $0.5 \times 10^{22} \text{ cm}^{-2}$, a typical value for LS I +61 303 also found in the *XMM-Newton* fits.

To look for short-term X-ray variability we also extracted 0.3–10 keV background-subtracted lightcurves for each observation. In addition we computed hardness ratios as the fraction between the count rates above and below 2 keV. More information about the X-ray analysis can be found in [17].

B. X-ray results & X-ray/TeV Correlation

There is no significant hardness ratio change within each of our observations. Thus the unabsorbed flux obtained from the spectral fit is a good estimate of the unabsorbed flux during the observation. Still moderate ($\Delta F < 25\%$) count-rate variability is present in most observations. We converted this count-rate variability into flux variability and added this flux variability (as an estimate of additional flux uncertainty) in quadrature to the spectral fits flux errors. This procedure provides more realistic total flux uncertainties.

We show in Fig. 2-bottom the 0.3–10 keV lightcurve of LS I +61 303 together with the VHE lightcurve obtained with MAGIC. A clear correlation between

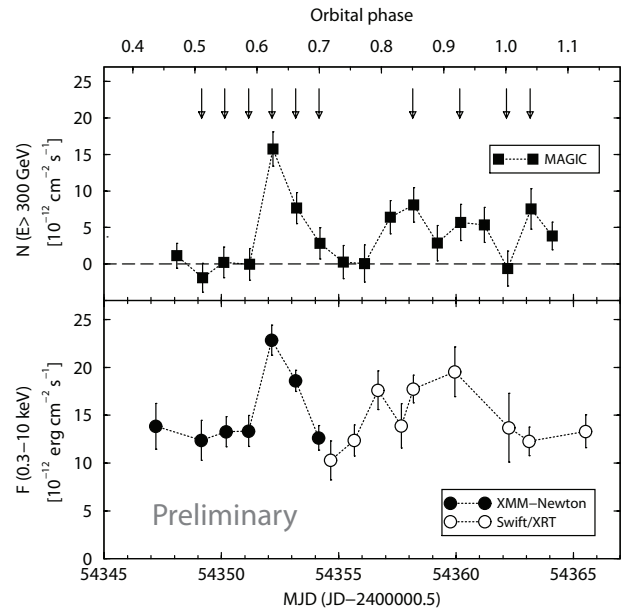


Fig. 2: TeV and X-ray lightcurves of LS I +61 303 during the multiwavelength campaign of 2007 September. *Top*: Flux above 300 GeV versus the observation time in MJD and the orbital phase. The horizontal dashed line indicates 0 flux. The vertical arrows mark the times of simultaneous TeV and X-ray observations. *Bottom*: Unabsorbed flux in the 0.3–10 keV energy range for the seven *XMM-Newton* observations (filled circles) and the nine *Swift* ones (open circles). Error bars correspond to a $1\text{-}\sigma$ confidence level in all cases. Dotted lines join consecutive data points to help following the main trends of the lightcurves.

the X-ray and TeV emissions is observed with a simultaneous peak at phase 0.62 (see Fig. 2). We plot in Fig. 3 the X-ray fluxes against the TeV fluxes for strictly simultaneous taken data, amounting to 10 data points (marked with arrows in Fig. 2). A linear fit to the six MAGIC/*XMM-Newton* pairs that trace the outburst yields a correlation coefficient of $r = 0.97$. A linear fit to all ten simultaneous pairs provides a high correlation coefficient of $r = 0.81^{+0.06}_{-0.21}$ (which has a probability of about 5×10^{-3} to be produced from independent X-ray and TeV fluxes).

Contemporaneous radio data obtained with RATAN, VLBA and $H\alpha$ spectroscopy, are consistent with previous result (details will be reported elsewhere). Therefore, the X-ray/TeV correlation occurred when the source was showing a standard behavior in both its outflow (radio) and decretion disk ($H\alpha$ line).

VI. CONCLUSION

We find that LS I +61 303 is a periodic γ -ray binary with an orbital period of 26.8 ± 0.2 days (chance probability $\sim 10^{-7}$), compatible with the optical, radio and X-ray period. This result implies that the flux modulation is tied to the orbital period.

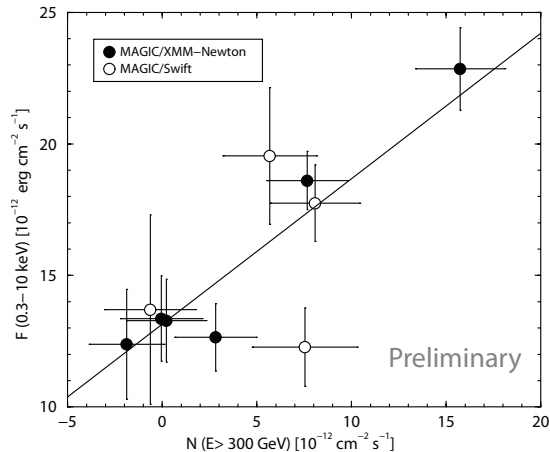


Fig. 3: Unabsorbed X-ray fluxes as a function of TeV fluxes for LS I +61 303 during the multiwavelength campaign of 2007 September. Only the 10 simultaneous fluxes, marked with arrows in Fig. 2, have been considered. Filled circles represent *XMM-Newton* measurements, while open ones are those from *Swift*. Error bars correspond to a $1\text{-}\sigma$ confidence level in all cases. The solid line represents a linear fit to all data points.

We produce energy spectra for several phase bins and the spectral photon index does not show a significant dependence on the orbital phase.

We put constraints to the emission at the periastron passage and conclude that the system is detected in γ -rays only in the phases 0.4 – 1.0. Since significant emission is only detected in an orbital sector off the phases at which the maximum gamma ray flux should occur under photon-photon absorption, the latter can hardly be the only source of variability in the emission.

In addition we have discovered an X-ray/TeV correlation in LS I +61 303 based on simultaneous multiwavelength data obtained with MAGIC, *XMM-Newton*, and *Swift*. The quoted X-ray fluxes are already unabsorbed and the TeV spectra show no absorption indication nor is significant absorption predicted for the explored phase range. Therefore, the X-ray/TeV correlation we have found for LS I +61 303 indicates that the emission processes at both wavelengths occur at the same time and are probably the result of a single physical mechanism.

Since the VHE flux is about a factor of 2 lower than the X-ray flux measured the X-ray/TeV correlation favor leptonic models if the radiation mechanisms are dominated by a single particle population. In addition, the IC cooling channel is less efficient than the synchrotron channel to produce the detected X-ray emission for reasonable values of the magnetic field. This suggests that the X-rays are the result of synchrotron radiation of the same VHE electrons that produce TeV emission as a result of inverse Compton scattering of optical/ultraviolet stellar photons.

ACKNOWLEDGMENTS

We thank N. Gehrels for his help in arranging the *Swift* observations. We would like to thank the Instituto de Astrofísica de Canarias for the excellent working conditions at the Observatorio del Roque de los Muchachos in La Palma. The support of the German BMBF and MPG, the Italian INFN and Spanish MICINN is gratefully acknowledged. This work was also supported by ETH Research Grant TH 34/043, by the Polish MNiSzW Grant N N203 390834, and by the YIP of the Helmholtz Gemeinschaft.

REFERENCES

- [1] D. A. Frail and R. M. Hjellming, “Distance and total column density to the periodic radio star LSI + 61° 303,” *The Astrophysical Journal*, vol. 101, pp. 2126–2130, Jun. 1991.
- [2] J. Casares *et al.*, “Orbital parameters of the microquasar Lsi +61 303,” *Mon. Not. Roy. Astron. Soc.*, vol. 360, pp. 1091–1104, 2005.
- [3] E. D. Grundstrom *et al.*, “Joint H α and X-Ray Observations of Massive X-Ray Binaries. II. The Be X-Ray Binary and Microquasar LS I +61 303,” *The Astrophysical Journal*, vol. 656, pp. 437–443, Feb. 2007.
- [4] C. Aragona *et al.*, “Optical Spectroscopy of Gamma-ray Binaries,” in *American Astronomical Society Meeting Abstracts*, ser. American Astronomical Society Meeting Abstracts, vol. 213, Jan. 2009, pp. 410.08–.
- [5] M. Massi *et al.*, “Hints for a fast precessing relativistic radio jet in LS I +61°303,” *Astronomy & Astrophysics*, vol. 414, pp. L1–L4, Jan. 2004.
- [6] V. Dhawan, A. Mioduszewski, and M. Rupen, “LS I +61 303 is a Be-Pulsar binary, not a Microquasar,” in *Proceedings of the VI Microquasar Workshop: Microquasars and Beyond. September 18-22, 2006, Como, Italy.*, p.52.1, 2006.
- [7] J. Albert *et al.*, “Multiwavelength (Radio, X-Ray, and γ -Ray) Observations of the γ -Ray Binary LS I +61 303,” *The Astrophysical Journal*, vol. 684, pp. 1351–1358, Sep. 2008.
- [8] G. Dubus, “Gamma-ray absorption in massive X-ray binaries,” *Astronomy & Astrophysics*, vol. 451, pp. 9–18, May 2006.
- [9] P. C. Gregory, “Bayesian Analysis of Radio Observations of the Be X-Ray Binary LS I +61°303,” *The Astrophysical Journal*, vol. 575, pp. 427–434, Aug. 2002.
- [10] A. Smith *et al.*, “Long-Term X-Ray Monitoring of the TeV Binary LS I +61 303 With the Rossi X-Ray Timing Explorer,” *The Astrophysical Journal*, vol. 693, pp. 1621–1627, Mar. 2009.
- [11] J. Albert *et al.*, “Variable very high energy gamma-ray emission from the microquasar LS I +61 303,” *Science*, vol. 312, pp. 1771–1773, 2006.
- [12] J. Albert *et al.*, “Periodic Very High Energy γ -Ray Emission from LS I +61° 303 Observed with the MAGIC Telescope,” *The Astrophysical Journal*, vol. 693, pp. 303–310, Mar. 2009.
- [13] V. A. Acciari *et al.*, “VERITAS Observations of the γ -Ray Binary LS I +61 303,” *The Astrophysical Journal*, vol. 679, pp. 1427–1432, Jun. 2008.
- [14] V. A. Acciari *et al.*, “Multiwavelength Observations of LS I +61 303 with VERITAS, Swift and RXTE,” *ArXiv e-prints*, Apr. 2009.
- [15] E. Aliu *et al.*, “Improving the performance of the single-dish Cherenkov telescope MAGIC through the use of signal timing,” *Astroparticle Physics*, vol. 30, pp. 293–305, Jan. 2009.
- [16] J. Albert *et al.*, “VHE γ -Ray Observation of the Crab Nebula and its Pulsar with the MAGIC Telescope,” *The Astrophysical Journal*, vol. 674, pp. 1037–1055, Feb. 2008.
- [17] —, “in preparation.”
- [18] J. D. Scargle, “Studies in astronomical time series analysis. II - Statistical aspects of spectral analysis of unevenly spaced data,” *The Astrophysical Journal*, vol. 263, pp. 835–853, Dec. 1982.
- [19] K. A. Arnaud, “XSPEC: The First Ten Years,” in *Astronomical Data Analysis Software and Systems V*, ser. Astronomical Society of the Pacific Conference Series, G. H. Jacoby and J. Barnes, Eds., vol. 101, 1996, pp. 17–.